Electronic Supplementary Information

Substrate-induced assembly of cascade enzymes and catalytic surfactants: nanoarchitectonics at the oil-in-water droplet interface

Priyanka, Manpreet Kaur, Subhabrata Maiti*

Department of Chemical Sciences, Indian Institute of Science Education and Research (IISER) Mohali, Knowledge City, Manauli 140306, India.

E-mail: smaiti@iisermohali.ac.in

Table of Content

1. Materials, Methods and Synthetic protocols:

All commercially available reagents were used as received without any further purification. The chemicals sodium phosphate dibasic (Na_2HPO_4), hexadecyl bromide ($C_{16}H_{33}Br$), Fluorescein isothiocyanate (FITC), HEPES (4-(2-hydroxyethyl)-1-piperazineethanesulfonic acid), 1,2 – dichlorobenzene, N, N'-Dicyclohexylcarbodiimide (DCC), 4-Dimethylaminopyridine (DMAP), Glucose, enzyme Horseradish Peroxidase Type 2 (HRP) and Glucose Oxidase from Aspergillus Niger (GOx) were procured from Sisco Research Laboratory (SRL), India. 1,9-Dibromononane, potassium thioacetate, di-(2-picolyl)amine (DPA), coumarin-343, Tetramethylrhodamine isothiocyanate were (TRITC), and DMSO were purchased from Sigma-Aldrich. Resorufin was purchased from TCI Chemicals India. Amplex Red was purchased from Invitrogen. The chemicals potassium carbonate (K_2CO_3), and potassium iodide (KI), were also purchased from SRL India, and magnesium nitrate was obtained from Molychem. HPLC-grade methanol and acetonitrile purchased from Sigma-Aldrich were used in the synthesis.

Reactions were monitored by thin layer chromatography (TLC) using silica aluminium sheets with fluorescent indicator at 254 nm (Aldrich). Column Chromatography was performed with 60 - 120 mesh silica gel and neutral alumina. ^1H and ^{13}C NMR spectra were recorded respectively on Bruker 400 MHz and 100 MHz NMR spectrometer using $CDCl_3$. Chemical shifts (δ) are given in ppm with TMS as an internal reference. *J* values are given in Hertz (Hz). High-resolution mass spectra (HRMS) were recorded on Waters QTOF mass spectrometer.

Stock solutions of enzyme/dye were prepared both by weight and by UV–visible spectroscopy using molar extinction ε_{280} (HRP) = 102 000 $M^{-1}cm^{-1}$, ε_{259} (ATP) = 15400 $M^{-1}cm^{-1}$, ε_{485} (TRITC) = 62100 $M^{-1}cm^{-1}$, ε_{495} (FITC) = 68000 $M^{-1}cm^{-1}$, ε_{280} (GOx) = 220800 $M^{-1}cm^{-1}$. UV-vis studies were performed using a Varian Cary 60 (Agilent Technologies) spectrophotometer.

Fluorescence measurements were performed using Cary Eclipse Fluorescence Spectro-fluorometer.

All fluorescence microscopy imaging was performed on ZEISS LSM 980 Elyra 7 super-resolution Microscope using a ×63 oil-immersion objective (N.A. 1.4) and a monochrome cooled high-resolution AxioCamMRm Rev. 3 FireWire(D) camera.

The surfactant $C_{16}DPA{\bullet}Zn^{2+}$ and substrate HPNPP was synthesized and characterized as reported in the literature.[S1]

HPLC condition: The HPLC analyses were performed using an Agilent 1260 Infinity II HPLC, equipped with a diode array detector (DAD), (λ_{det} = 255 nm, 290 nm and 315 nm). Conditions: Flow rate: 0.5 ml/min, Isocratic Gradient: 50 % of A - 50 % of B (A: H2O+0.1% HCOOH, B: ACN+0.1% HCOOH) from 0 to 10min. Column: C18, 4µm, 150×4.6mm column. The injection volume was 20 µl. The temperature of the column was 25°C.

Oil-in-water Droplet formation: For the Oil in water droplet, we used 20 µl of 1,2-dichlorobenzene in 980 µl of 5 mM HEPES Buffer pH7 in the presence of 250 µM $C_{16}DPA{\bullet}Zn^{2+}$. 2% of 1,2-dichlorobenzene was used during oil in water droplet formation. The mixed solution was vortexed for 60s, which resulted in the formation of micron-sized oil in water droplets.

During the cascade reactions, all the constituents were added along with the surfactant before vortexing, Similarly, during HPNPP catalysis, HPNPP was added before vortexing along with the surfactant and oil.

Preparation of FITC Tagged ALP

FITC-tagged ALP was prepared as given in the literature.[S2] 1 mg/ml of FITC was dissolved in DMSO, then 100 µl of this was mixed with 5 mg/ml of ALP (prepared in 0.1M sodium carbonate bicarbonate buffer of pH 9). For five to six hours, the solution was stored at 4 °C in the dark. Subsequently, 100 µl of 50 mM ammonium chloride was added to quench the continuing tagging reaction, and the mixture was left for over two hours. After that, the reaction mixture was run through a Sephadex G-25 column, and 5 mM HEPES buffer (pH=7) was used to purify the conjugate that had produced. Following collection of the eluted samples in several vials, the UV absorption spectra of the conjugate of FITC and ALP were recorded, revealing FITC at 495 nm and absorption maxima at 280 nm peak. The ALP tagging efficiency was determined to be 0.9, indicating an average of 0.9 FITC molecule for a single enzyme.

Preparation of TRITC tagged GOx

TRITC tagged GOx was prepared as given in the literature.[S2] 1 mg/ml TRITC was dissolved in DMSO, and then 100 µl of this was mixed with 6 mg/ml of GOx (prepared in 0.1M sodium carbonate bicarbonate buffer of pH 9). For five to six hours, the solution was stored at 4 °C in the dark. Subsequently, 100 µl of 50 mM ammonium chloride was added to quench the continuing tagging reaction, and the mixture was left for over two hours. After that, the reaction mixture was run through a Sephadex G-25 column, and 5 mM HEPES buffer (pH=7) was used to purify the conjugate that had produced. Following collection of the eluted samples in several vials, the UV absorption spectra of the conjugate of TRITC and GOx were recorded, revealing TRITC at 522 nm and absorption maxima at 280 nm peak. The GOx tagging

efficiency was determined to be 2, indicating an average of 2 TRITC molecule for a single enzyme.

Preparation of TRITC Tagged HRP

TRITC tagged HRP was prepared as given in literature.[S2] 1 mg/ml TRITC was dissolved in DMSO, then 100 µl of this was mixed with 6 mg/ml of HRP (prepared in 0.1M sodium carbonate bicarbonate buffer of pH 9). For five to six hours, the solution was stored at 4 °C in the dark. Subsequently, 100 µl of 50 mM ammonium chloride was added to quench the continuing tagging reaction, and the mixture was left for over two hours. After that, the reaction mixture was run through a Sephadex G-25 column, and 5 mM HEPES buffer (pH=7) was used to purify the conjugate that had produced. Following collection of the eluted samples in several vials, the UV absorption spectra of the conjugate of TRITC and HRP were recorded, revealing FITC at 522 nm and absorption maxima at 406 nm peak. The HRP tagging efficiency was determined to be 0.6, indicating an average of 0.6 FITC molecule for a single enzyme.

FRET Imaging via Acceptor Photobleaching

Metallomicelle enzyme conjugates were photographed with a ZEISS LSM 980 Elyra 7 super-resolution microscope using a 63x oil-immersion objective (N.A 1.4) and a monochrome-cooled high-resolution AxioCamMRm Rev. 3 FireWire(D) camera. The FRET efficiency was measured by photobleaching the acceptor in a dual-labeled surfactant stabilised o/w interface using a 560 nm laser. Following the bleaching of the acceptor fluorophore, an increase in donor fluorescence intensity was observed.

To assess the FRET efficiency, ZEISS (Zen Blue 3.2) software was utilised. Using the built-in software, the FRET efficiency (FRETeff) was determined in accordance with the following equation[S3]:

$$FRET_{eff}=[D_{post}-D_{pre}]/Dpost$$

Donor fluorescence before photobleaching is denoted by Dpre, and donor fluorescence following photobleaching is denoted by Dpost.
After calibrating the photos, the intensity profile data with respect to distance was gathered using ImageJ software.

Synthetic protocol

Reaction scheme

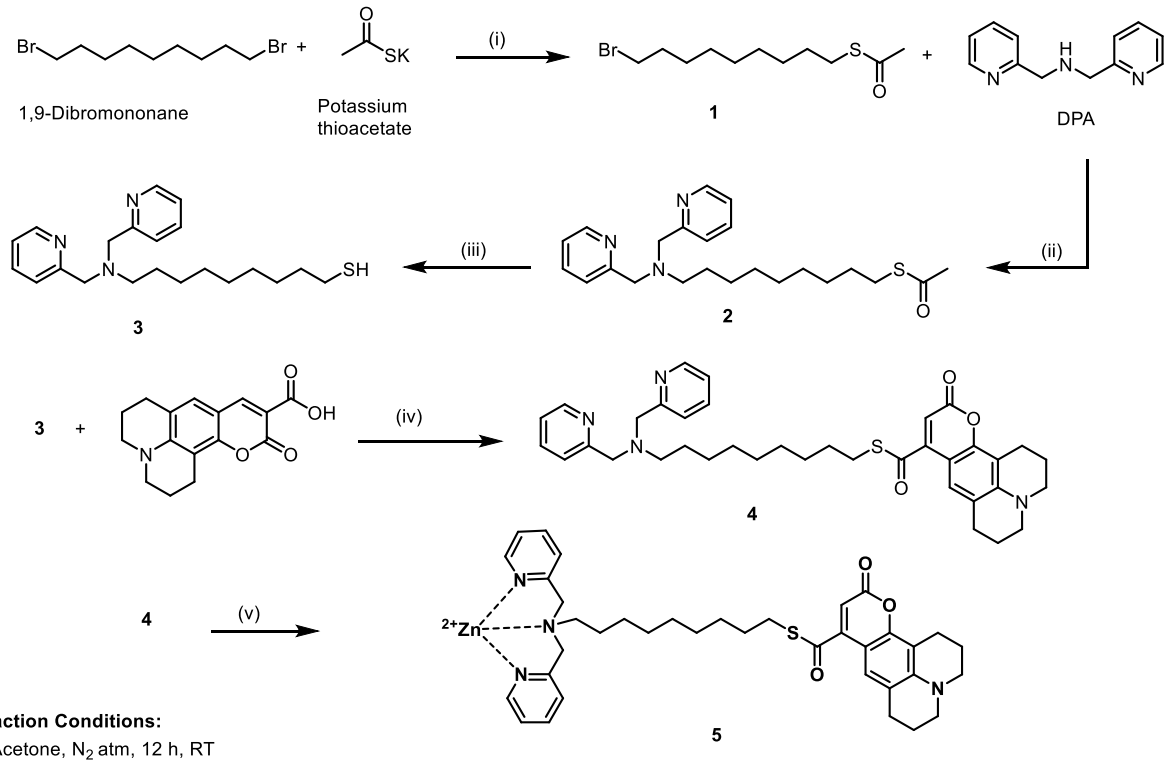

Reaction Conditions:
(i) Acetone, N_2 atm, 12 h, RT
(ii) $NaHCO_3$, K_2CO_3, ACN, 60 ^oC, 24 h
(iii) MeOH, 6 M HCl, 60 ^oC, 4h
(iv) DCC, DMAP, dry DCM, 12 h, RT
(v) $Zn(NO_3)_2$, MeOH, reflux, 12 h

Synthesis of S-(9-bromononyl) ethanethioate (1)

Compound **1** was synthesized by first dissolving 1,9-dibromononane (1 g, 3.49 mmol) in 15 mL of distilled acetone in a round bottom flask and to this potassium thioacetate (0.39 g, 3.49 mmol) was added. The reaction mixture was allowed to stir at room temperature for 12 h under N_2 atm. The resulting suspension formed was filtered using suction filtration and the filtrate was then evaporated on rotary evaporator to yield crude product as thick oil. The crude was further purified via silica gel (60-120 mesh) column chromatography using hexane as eluent to procure compound **1** as colorless oil with 49% yield.

^{1}H NMR (400MHz, $CDCl_3$) δ: 3.42 (t, *J* = 6.8 Hz, 2H), 2.87 (t, *J* = 7.2 Hz, 2H), 2.33 (s, 3H), 1.90-1.83 (m, 2H), 1.61-1.54 (m, 2H), 1.45-1.31 (m, 10H).

^{13}C NMR (100 MHz, $CDCl_3$) δ: 196.0. 77.2, 34.0, 32.7, 30.6, 29.4, 29.2, 29.1, 28.9, 28.7, 28.6, 28.1.

Synthesis of S-(9-(bis(pyridin-2-ylmethyl)amino)nonyl) ethanethioate (2)

Compound **1** (0.3 g, 1.06 mmol) was added to a suspension of dipicolylamine (0.212 g, 1.06 mmol), potassium carbonate (0.441 g, 3.20 mmol) and sodium bicarbonate (0.268 g, 3.20 mmol) in acetonitrile (10 mL). The reaction mixture was stirred at 60 ^oC for 24 h; after the completion of reaction, the resulting suspension was filtered. The evaporation of the filtrate gave crude product which was further purified via silica gel (60-120 mesh) column chromatography using ethyl acetate/hexane. Yellow oil; yield 40%.

^{1}H NMR (400 MHz, $CDCl_3$) δ: 8.50 (d, *J* = 4.3 Hz, 2H), 7.63 (t, *J* = 7.7 Hz, 2H), 7.53 (d, *J* = 7.8 Hz, 2H), 7.12 (t, *J* = 5.8 Hz, 2H), 3.79 (s, 4H), 3.47 (s, MeOH), 2.83 (t, *J* = 7.32 Hz, 2H), 2.51 (t, *J* = 7.2 Hz, 2H), 2.30 (s, 3H), 1.54-1.49 (m, 4H), 1.32-1.20 (m, 10H).

^{13}C NMR (100 MHz, $CDCl_3$) δ: 196.0, 160.1, 148.9, 136.3, 122.8, 121.8, 77.32, 60.5, 54.5, 30.6, 29.4, 29.3, 29.1, 29.0, 28.7.

Synthesis of 9-(Bis(pyridin-2-ylmethyl)amino)noname-1-thiol (3)

Compound **3** was synthesized by dissolving **2** (0.16 g, 0.40 mmol) in 5 mL MeOH in a 25 mL round bottom flask, and to this 5 mL of 6 M HCl was added. The reaction mixture was heated at 60 ^oC for 4 h and after evaporation of the solvent under reduced pressure, the aqueous part was neutralized with 2 M NaOH solution. Compound **3** was extracted using diethyl ether which after evaporation gave yellow oil as the pure product with 85% yield.

^{1}H NMR (400 MHz, $CDCl_3$) δ: 8.53 (d, *J* = 4.4 Hz, 2H), 7.68-7.64 (m, 2H), 7.55 (d, *J* = 7.8 Hz, 2H), 7.16 (t, *J* = 5.7 Hz, 2H), 3.82 (s, 4H), 2.54-2.47 (m, 4H), 2.08 (CH_3COCH_3), 1.60-1.50 (m, 4H), 1.33-1.21 (m, 10H).

^{13}C NMR (100 MHz, $CDCl_3$) δ: 159.6, 148.5, 136.6, 122.9, 122.0, 77.1, 59.9, 54.4, 33.9, 29.3, 29.2, 28.9, 28.2, 27.1, 26.8, 24.5, 20.8.

Synthesis of *S*-(9-(bis(pyridin-2-ylmethyl)amino)nonyl) 11-oxo-2,3,6,7-tetrahydro-1*H*,5*H*,11*H*-pyrano[2,3-*f*]pyrido[3,2,1-*ij*]quinoline-9-carbothioate (4)

To a solution of coumarin-343 (0.023 g, 0.08 mmol), DCC (0.051 g, 0.25 mmol) and DMAP (0.015 g, 0.12 mmol) in dry DCM, compound **3** (0.03 g, 0.08 mmol) was added. The resulting solution was allowed to stir at room temperature for 12 h. The progress of the reaction was monitored by shift in the UV-Vis absorption band from 450 nm to 420 nm. After evaporation of solvent under reduced pressure, the product was purified via column chromatography using neutral alumina. Yelow solid, yield 30%.

^{1}H NMR (400 MHz, $CDCl_3$) δ: 8.44 (d, *J* = 4.3 Hz, 2H), 8.14 (d, *J* = 6.2 Hz, 2H), 7.57 (t, *J* = 7.4 Hz, 2H), 7.48-7.46 (m, 2H), 7.06 (t, *J* = 6.1 Hz, 2H), 3.72 (s, 4H), 3.13-3.09 (m, 2H), 2.79-2.75 (m, 2H), 2.44 (t, *J* = 7.2 Hz, 2H), 2.24-2.22 (m, 2H), 1.85-1.83 (m, 4H), 1.67-1.65 (m, 4H), 1.50-1.43 (m, 4H), 1.24-1.18 (m, 10H).

^{13}C NMR (100 MHz, $CDCl_3$) δ: 196.1, 160.1, 154.2, 149.6, 148.9, 139.8, 136.3, 122.8, 121.8, 106.5, 77.2, 60.5, 55.7, 54.4, 39.0, 34.9, 30.6, 29.4, 29.3, 29.1, 29.0, 28.7, 27.2, 27.0, 25.4, 24.7.

HRMS (ESI): m/z calcd for $C_{37}H_{44}N_4O_3S$ $[M+H]^+$: 625.3206, found 625.3153.

NMR spectra

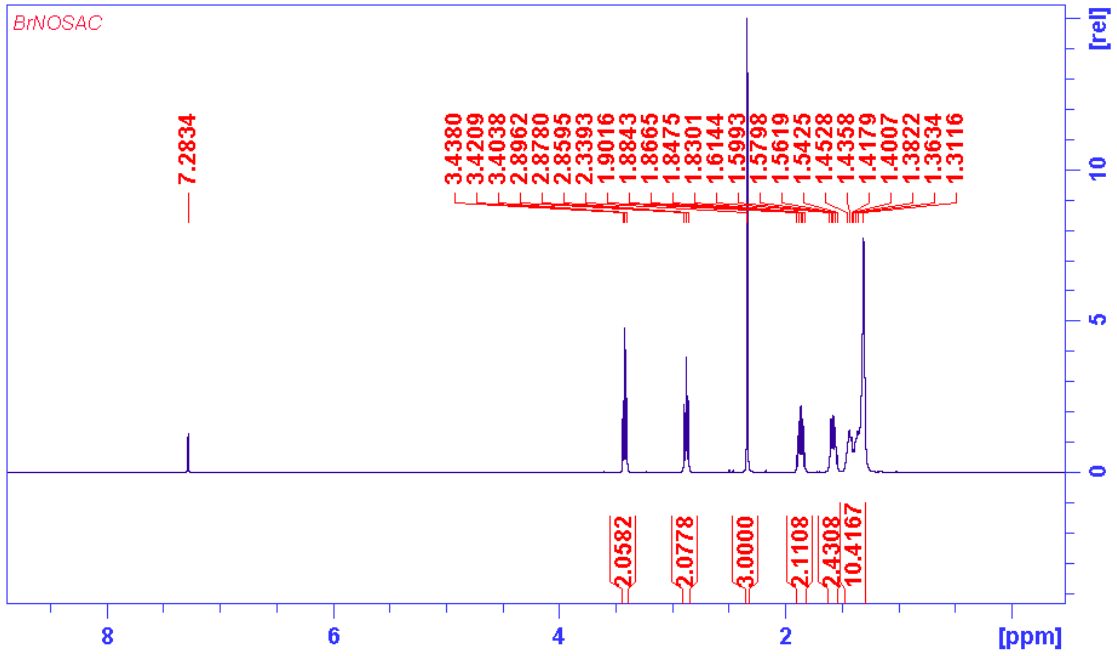

Fig. S1. ^{1}H NMR of compound **1** in $CDCl_3$.

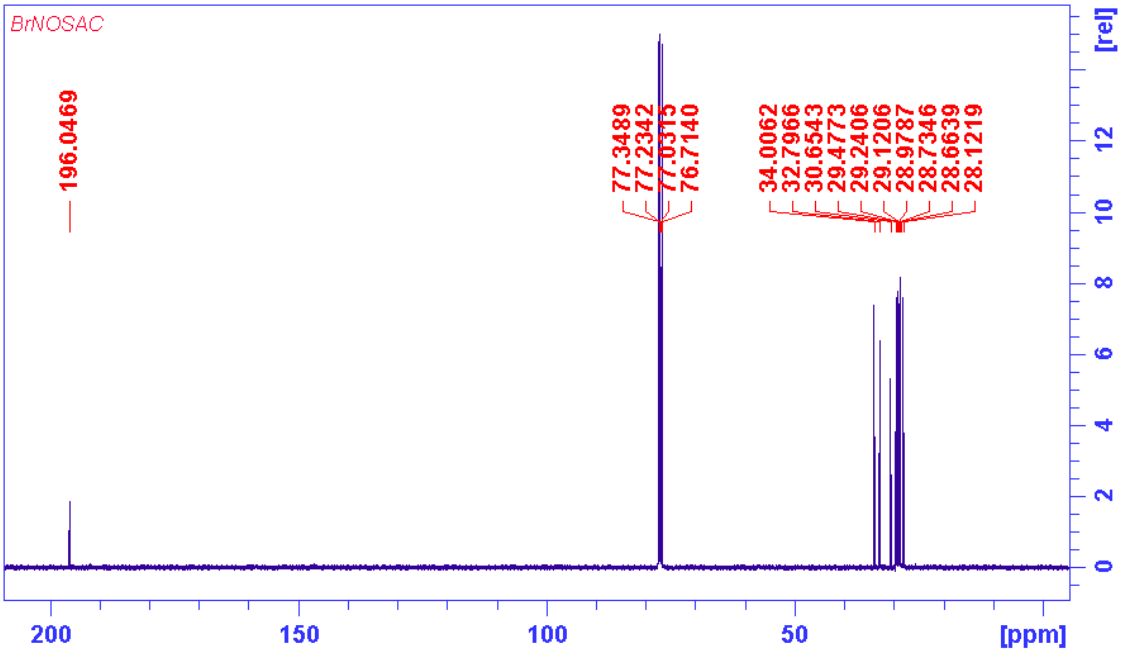

Fig. S2. ^{13}C NMR of compound **1** in $CDCl_3$.

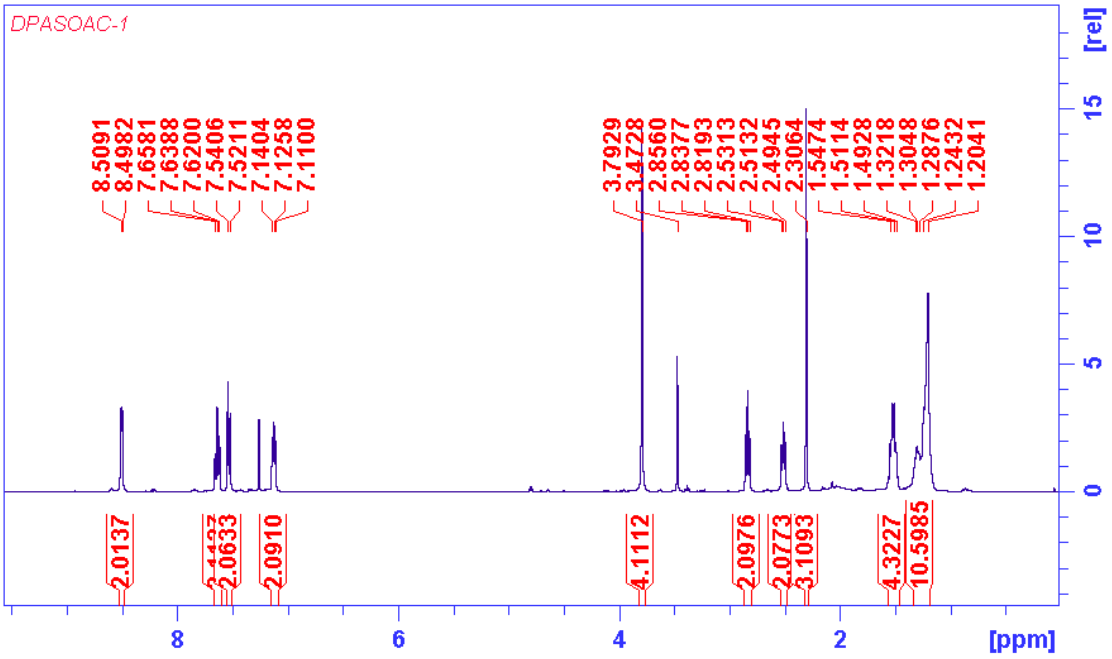

Fig. S3. ^{1}H NMR of compound **2** in $CDCl_3$.

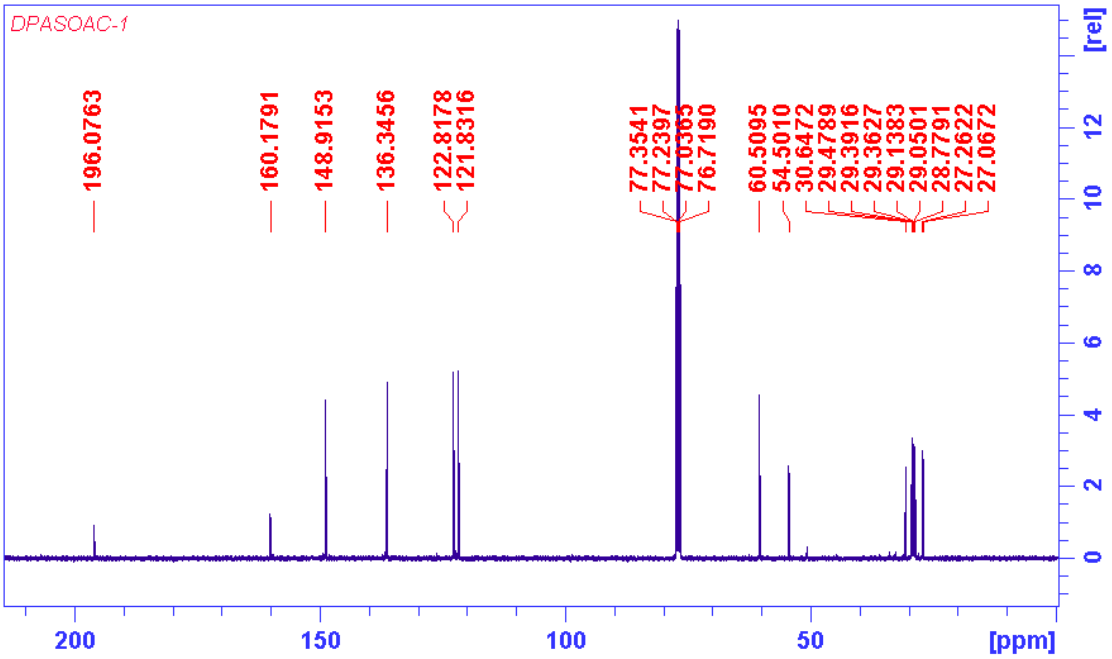

Fig. S4. ^{13}C NMR of compound **2** in $CDCl_3$.

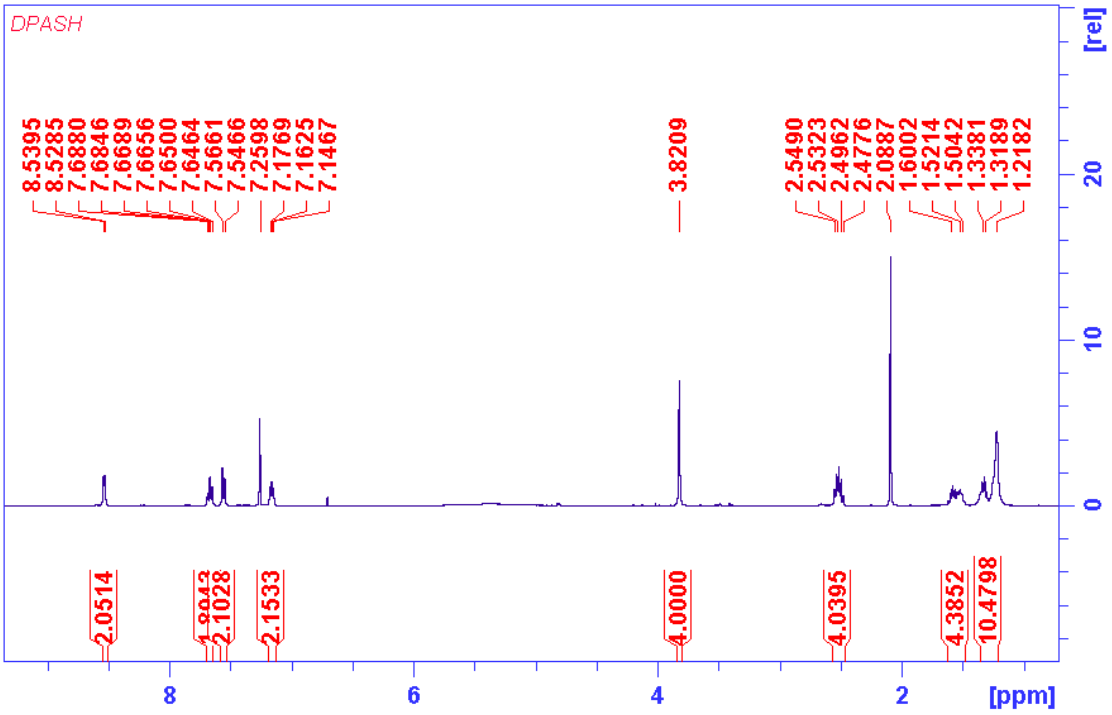

Fig. S5. ^{1}H NMR of compound **3** in $CDCl_3$.

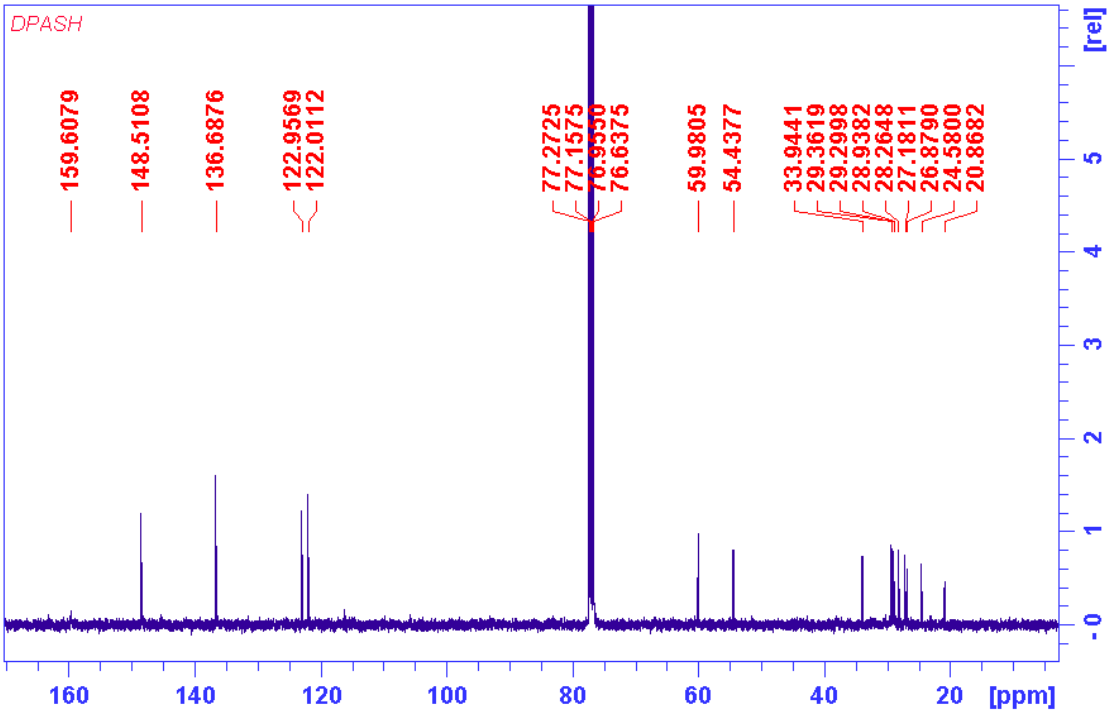

Fig. S6. ^{13}C NMR of compound **3** in $CDCl_3$.

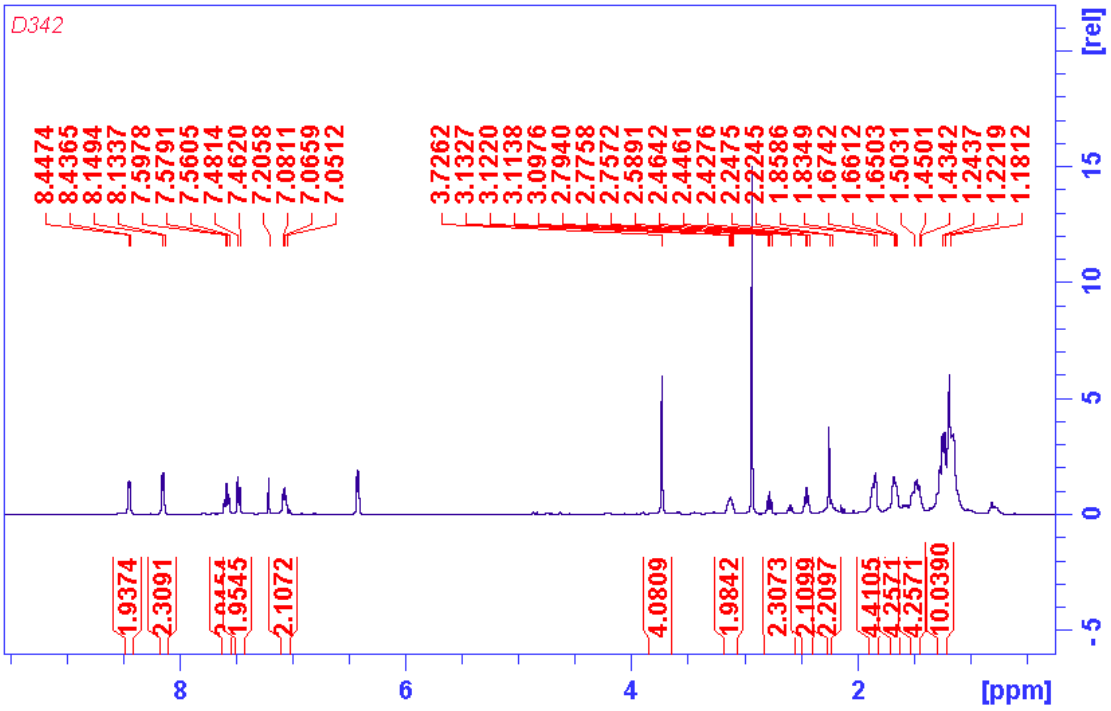

Fig. S7. ^{1}H NMR of compound **4** in $CDCl_3$.

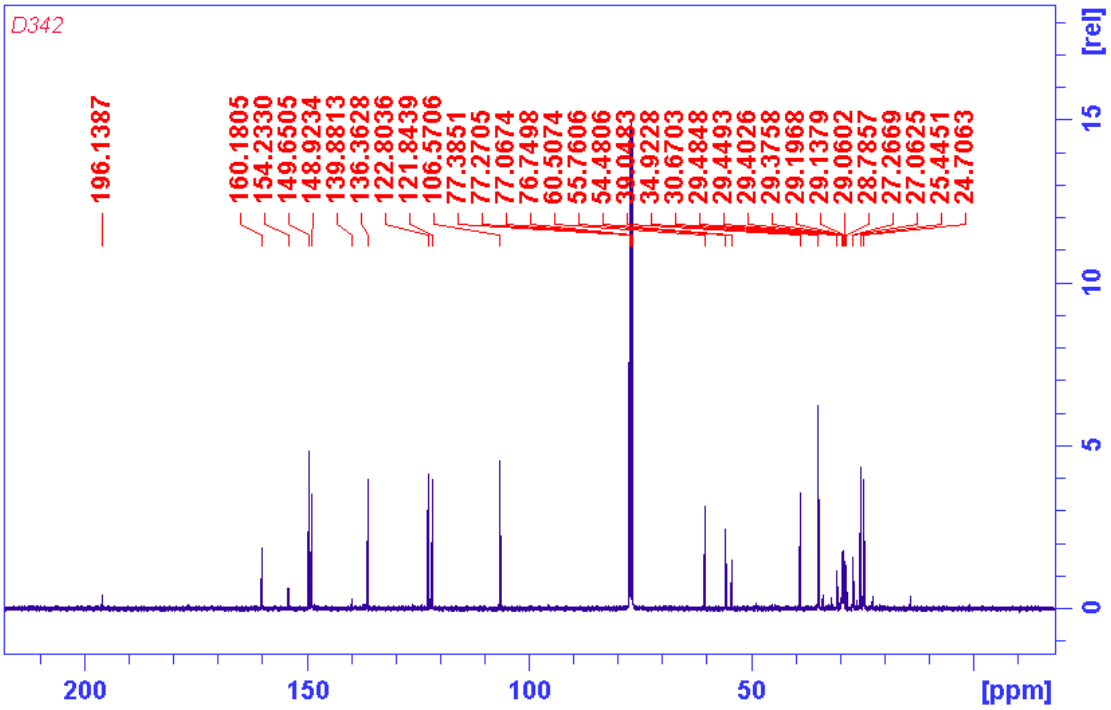

Fig. S8. ^{13}C NMR of compound **4** in $CDCl_3$.

Mass Spectra

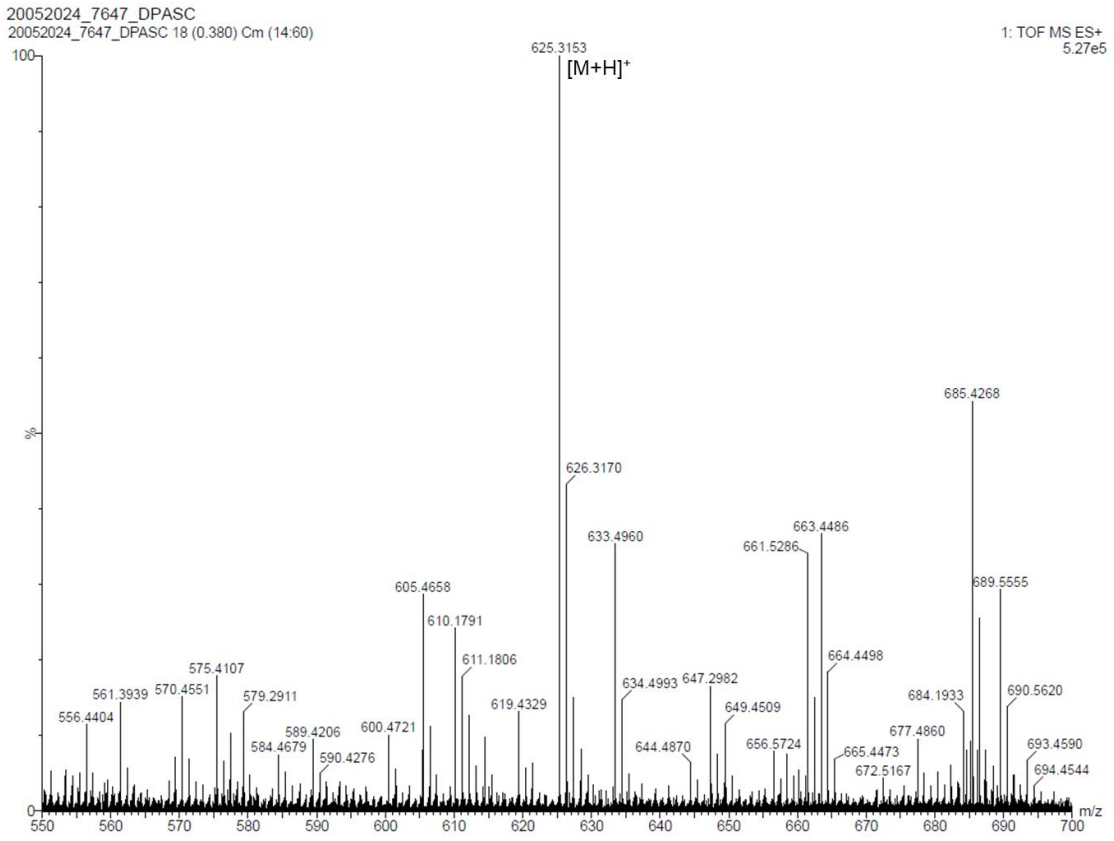

Fig. S9. HRMS of compound **4**, m/z calcd for $C_{37}H_{44}N_4O_3S$ $[M+H]^+$: 625.3206, found 625.3153.

2. Optical Microscopic Images:

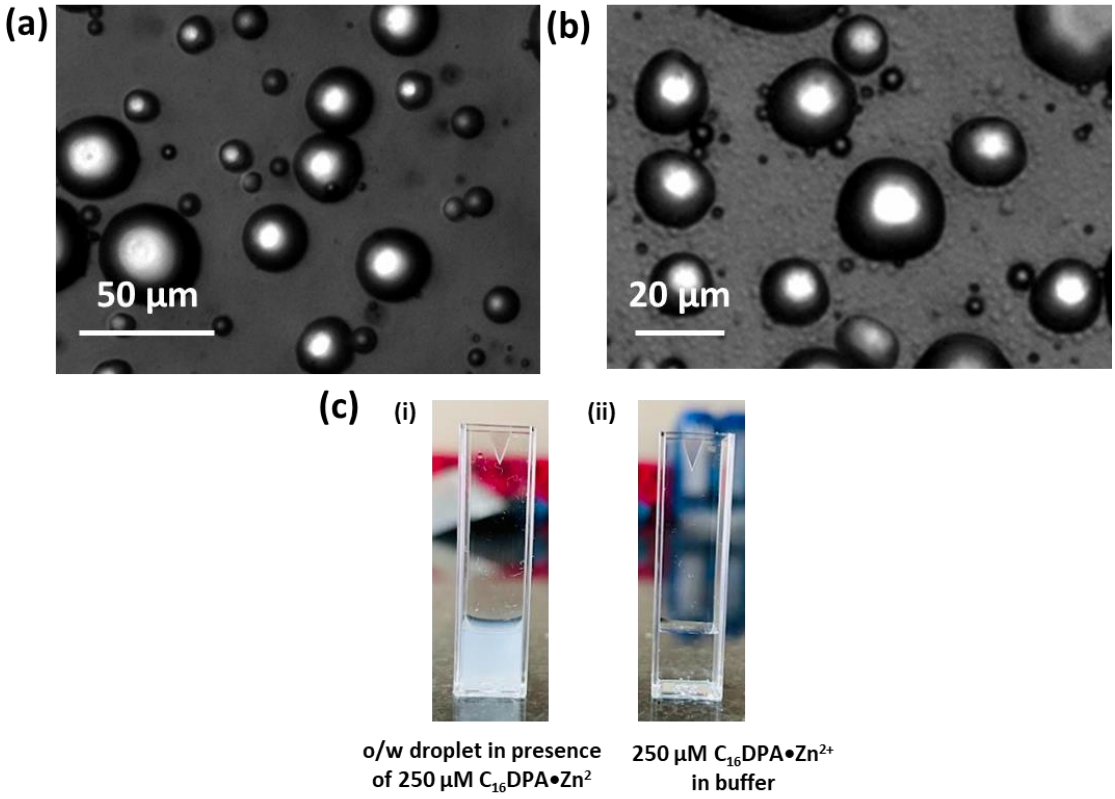

Fig. S10: (a) & (b) Representative Optical Microscopic Image of surfactant stabilized oil – in – water droplet. (c) Representative images of (i) oil in water droplet solution in the presence of 250 µM $C_{16}DPA•Zn^{2+}$ and (ii) only 250 µM $C_{16}DPA•Zn^{2+}$ solution in the buffer. Experimental Condition: [$C_{16}DPA•Zn^{2+}$] = 250 µM, [1,2-dichlorobenzene] = 20 µl in 980 µl 5mM HEPES buffer pH7 at 25°C.

3. Enzymatic Cascade Reaction Kinetics:

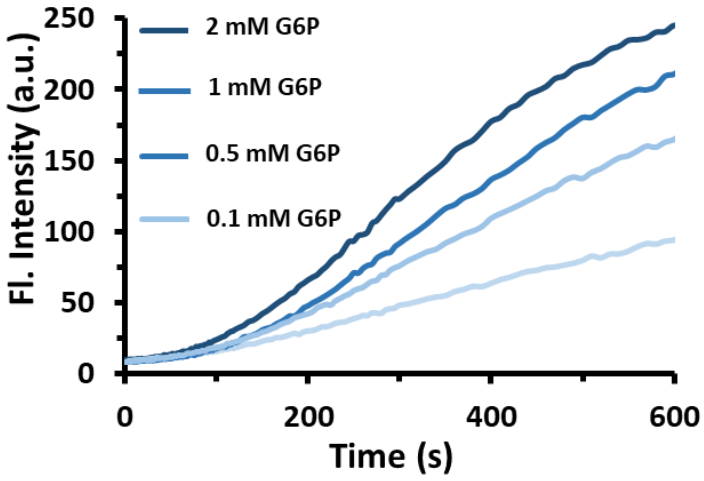

Fig. S11: Representative Fluorescence spectra of the formation of Resorufin over time in the cascade reaction with different conc. of substrate i.e G-6-P. Experimental Condition: [ALP] = 1 µM, [HRP] = 1 nM, [GOx] = 10 nM, [Amplex Red] = 10 µM, [G-6-P] = 0.1 - 2 mM, [C_{16}DPA•Zn^{2+}] = 250 µM, [1,2-dichlorobenzene] = 20 µl in 980 µl 5mM HEPES buffer pH7 at 25°C ex/em = 560/585 nm, ex/em slit width = 5/5.

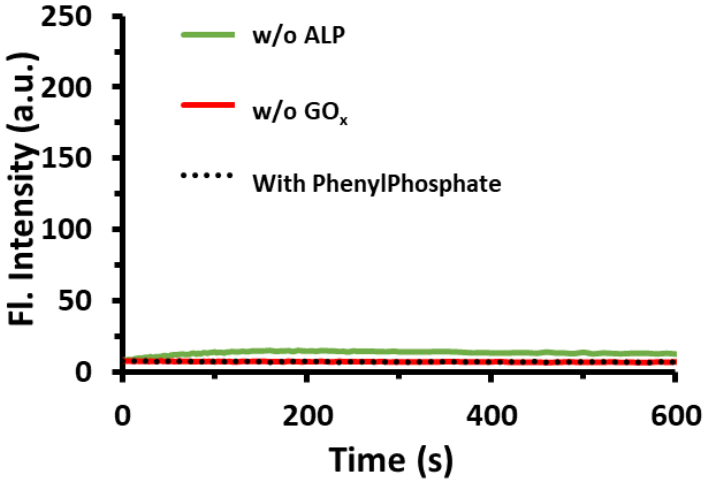

Fig. S12: Representative Fluorescence spectra of the formation of Resorufin over time in the control experiments of cascade reaction without ALP (green line), without GOx (red line), and with not relevant substrate i.e Phenyl phosphate (dotted black line) of the cascade enzymes. Experimental Condition: [ALP] = 1 µM, [HRP] = 1 nM, [GOx] = 10 nM, [Amplex Red] = 10 µM, [Phenylphosphate] = 1mM, [G-6-P] = 1 mM, [C_{16}DPA•Zn^{2+}] = 250 µM, [1,2-dichlorobenzene] = 20 µl in 980 µl 5mM HEPES buffer pH7 at 25°C ex/em = 560/585 nm, ex/em slit width = 5/5.

4. Binding of Enzymes on surfactant stabilized o/w interface :

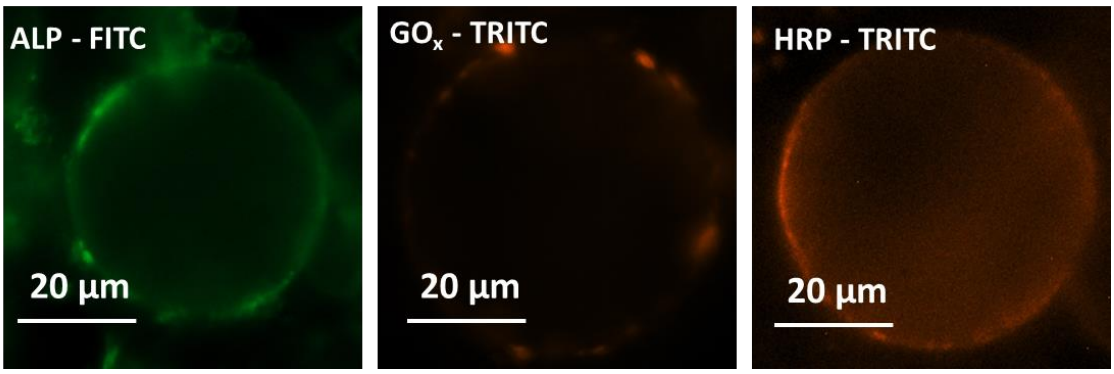

Fig. S13: Fluorescent microscopic images to show the binding of the fluorescently labeled enzymes, (ALP, GOx and HRP) used in this study at the interface. Here FITC and TRITC represent for fluorescein isothiocyanate and tetramethylrhodamine isothiocyanate, respectively. Experimental Condition: [ALP-FITC] = 1 µM, [HRP-FITC] = 0.5 µM, [GOx-FITC] = 0.5 µM [C_{16}DPA•Zn^{2+}] = 250 µM, [1,2-dichlorobenzene] = 20 µl in 980 µl 5mM HEPES buffer pH7 at 25°C.

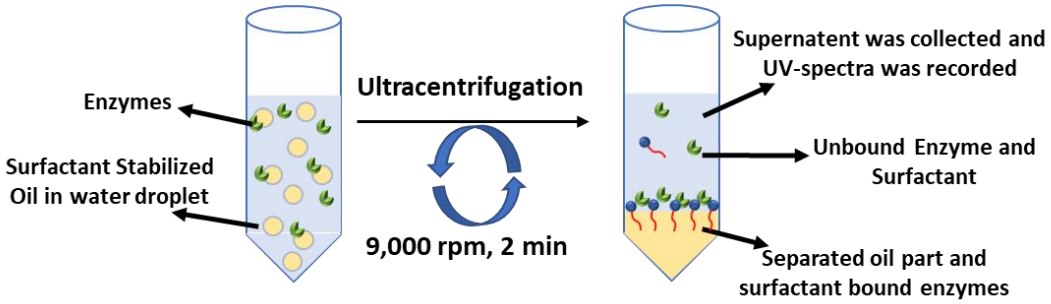

Fig. S14: Schematic representation for determination of bound enzymes at the o/w interface.

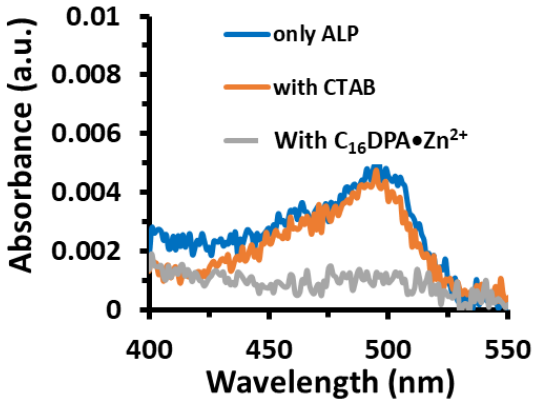

Fig. S15: Representative UV Spectra of the aqueous layer which represent unbound enzyme ALP- FITC after centrifugation of o/w droplet in the presence and absence of surfactants CTAB and C_{16}DPA•Zn^{2+}, in the system. Centrifugation was done at 9000 rpm for 2 minutes. Experimental Condition: [ALP-FITC] = 1 µM, [CTAB] = 250 µM, [C_{16}DPA•Zn^{2+}] = 250 µM, [1,2-dichlorobenzene] = 20 µl in 980 µl 5mM HEPES buffer pH7 at 25°C.

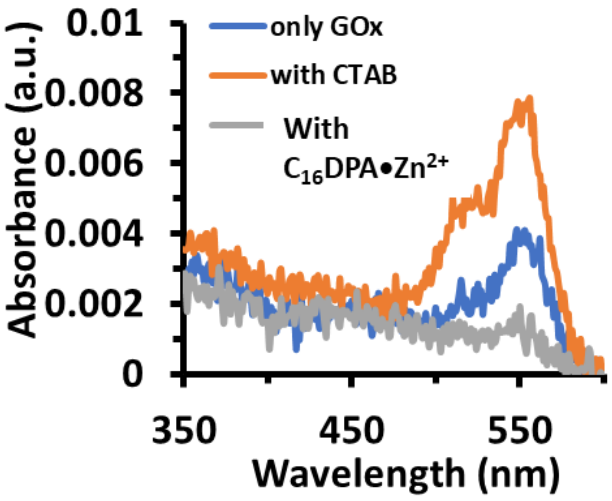

Fig. S16: Representative UV Spectra of the aqueous layer which represent unbound enzyme GOx - TRITC after centrifugation of o/w droplet in the presence and absence of surfactants CTAB and $C_{16}DPA•Zn^{2}$, in the system. Centrifugation was done at 9000 rpm for 2 minutes. Experimental Condition: [GOx-TRITC] = 1 µM, [CTAB] = 250 µM, [$C_{16}DPA•Zn^{2+}$] = 250 µM, [1,2-dichlorobenzene] = 20 µl in 980 µl 5mM HEPES buffer pH7 at 25°C.

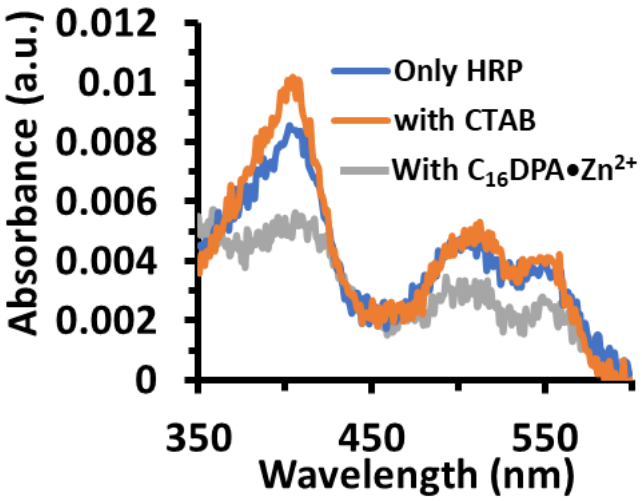

Fig. S17: Representative UV Spectra of the aqueous layer which represent unbound enzyme HRP-TRITC)after centrifugation of o/w droplet in the presence and absence of surfactants CTAB and $C_{16}DPA•Zn^{2}$, in the system. Centrifugation was done at 9000 rpm for 2 minutes. Experimental Condition: [HRP-TRITC] = 1 µM, [CTAB] = 250 µM, [$C_{16}DPA•Zn^{2+}$] = 250 µM, [1,2-dichlorobenzene] = 20 µl in 980 µl 5mM HEPES buffer pH7 at 25°C.

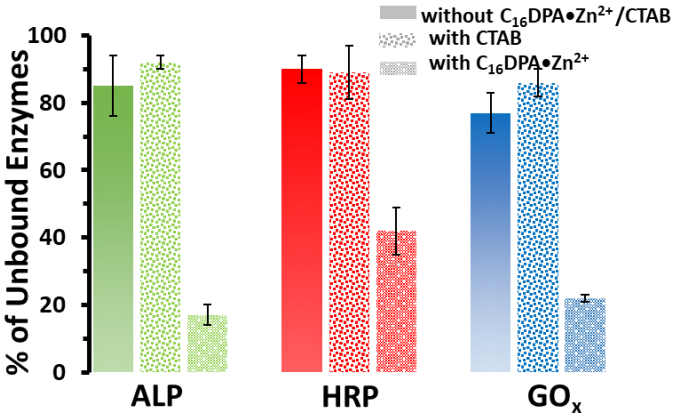

Fig. S18: Representative graph showing percentage of unbound enzymes which represent the amount of enzyme found in the aqueous layer after centrifugation of o/w droplet in the presence of CTAB, $C_{16}DPA•Zn^{2+}$ in the system. Error bars are the standard deviation of three independent experiments. Enzyme used 1 µM in each case. Experimental Condition: [ALP-FITC] = 1 µM, [GOx-TRITC] = 1 µM, [HRP-TRITC] = 1 µM, [CTAB] = 250 µM, [$C_{16}DPA•Zn^{2+}$] = 250 µM, [1,2-dichlorobenzene] = 20 µl in 980 µl 5mM HEPES buffer pH7 at 25°C.

This experiment revealed interfacial binding ability of ALP and GOx is around 80%, whereas for HRP it is close to 60%, in our experimental conditions.

5. **FRET Efficiency:**

(a) FRET Efficiency via Acceptor Photobleaching:

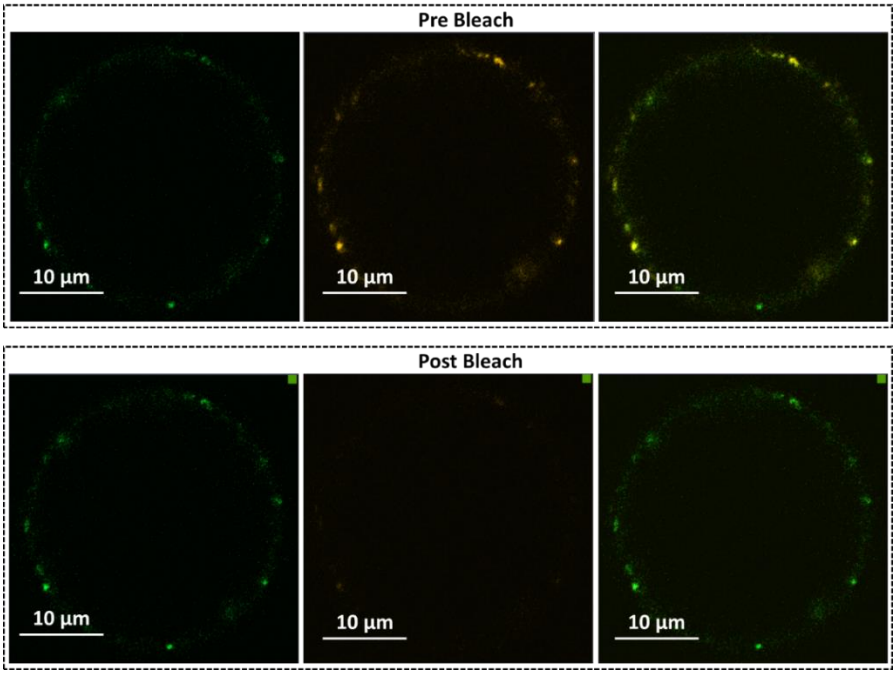

Fig. S19: Representative microscopic images of the surfactant stabilized o/w interface with FITC-ALP, TRITC-GOx and untagged HRP before and after photobleaching of TRITC. Experimental Condition : [ALP-FITC] = 1 µM, [GOx-TRITC] = 0.5 µM, [HRP] = 0.5 µM, [$C_{16}DPA•Zn^{2+}$] = 250 µM, [1,2-dichlorobenzene] = 20 µl in 980 µl 5mM HEPES buffer pH7 at 25°C.

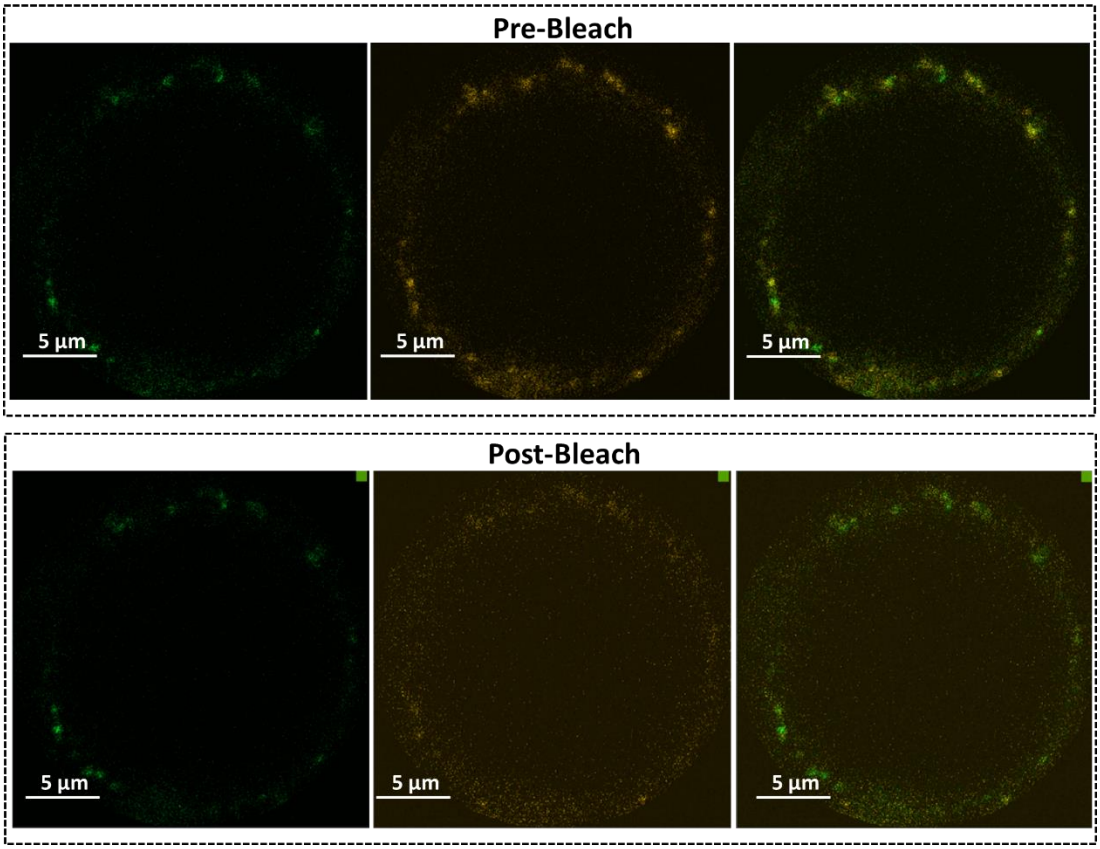

Fig. S20: Representative microscopic images of the surfactant stabilized o/w interface with FITC-ALP, TRITC-GOx and untagged HRP in the presence of Glucose + Phosphate before and after photobleaching of TRITC. Experimental Condition: [ALP-FITC] = 1 µM, [GOx-TRITC] = 0.5 µM, [HRP] = 0.5 µM, [C_{16}DPA•Zn^{2+}] = 250 µM, [Glucose] = 1 mM, [Na_2HPO_4] = 1 mM, [1,2-dichlorobenzene] = 20 µl in 980 µl 5mM HEPES buffer pH7 at 25°C.

(b) FRET Efficiency via Steady State Spectroscopy:

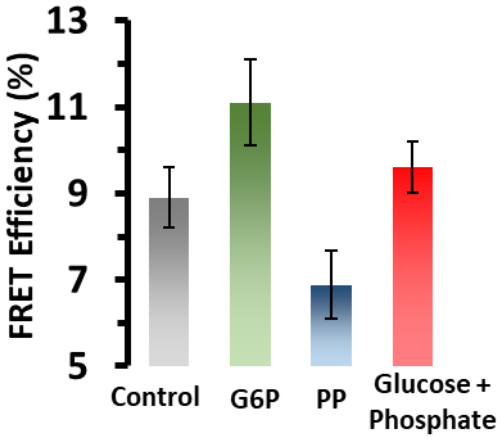

Fig. S21: FRET efficiency calculated from steady state fluorescence in the absence and presence of G-6-P, Glu + Pi and PP. Here we have used FITC tagged ALP, TRITC Tagged GOx, and untagged HRP during the FRET. Experimental condition: [ALP-FITC] = 1 µM, [GOx-TRITC] = 0.5 µM, [HRP] = 0.5 µM, [C_{16}DPA•Zn^{2+}] = 250 µM, [G-6-P] = 1 mM, [Phenyl Phosphate] = 1mM, [Glucose] = 1 mM, [Na_2HPO_4] = 1 mM, [1,2-dichlorobenzene] = 20 µl in 980 µl 5mM HEPES buffer pH7 at 25°C.

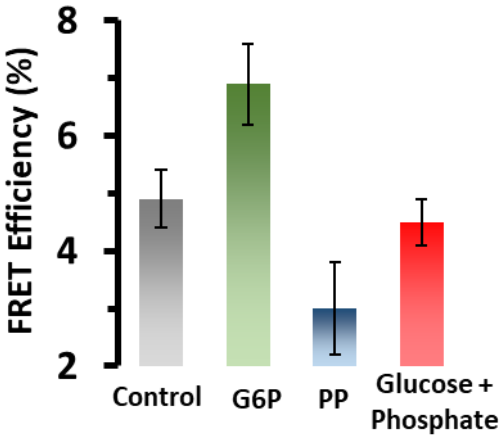

Fig. S22: FRET efficiency calculated from steady state fluorescence in the absence and presence of G-6-P, Glu + Pi and PP. Here we have used FITC tagged ALP, TRITC Tagged HRP, and untagged GOx during the FRET. Experimental condition: [ALP-FITC] = 1 µM, [HRP-TRITC] = 0.5 µM, [GOx] = 0.5 µM, [C_{16}DPA•Zn^{2+}] = 250 µM, [G-6-P] = 1 mM, [Phenyl Phosphate] = 1mM, [Glucose] = 1 mM, [Na_2HPO_4] = 1 mM, [1,2-dichlorobenzene] = 20 µl in 980 µl 5mM HEPES buffer pH7 at 25°C.

6. Two color confocal Microscopic Images:

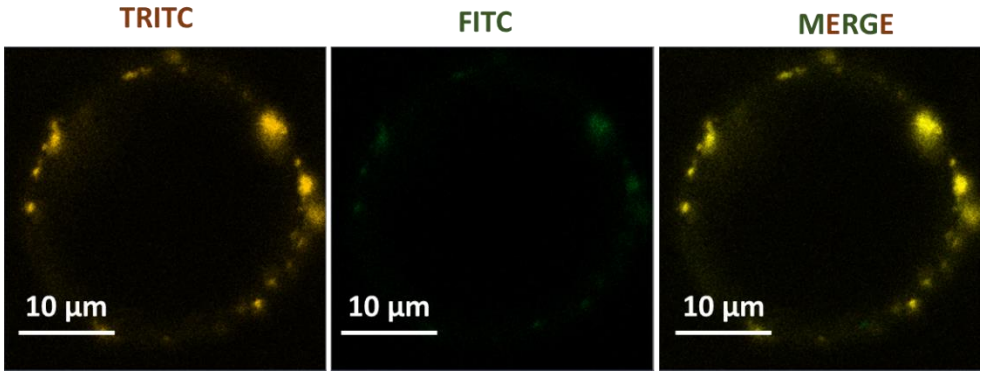

Fig. S23: Representative Two color images of surfactant stabilized o/w interface with GOx-TRITC, ALP-FITC and untagged HRP in the absence of substrate. Experimental condition: [ALP-FITC] = 1 µM, [GOx-TRITC] = 0.5 µM, [HRP] = 0.5 µM, [C_{16}DPA•Zn^{2+}] = 250 µM, [1,2-dichlorobenzene] = 20 µl in 980 µl 5mM HEPES buffer pH7 at 25°C.

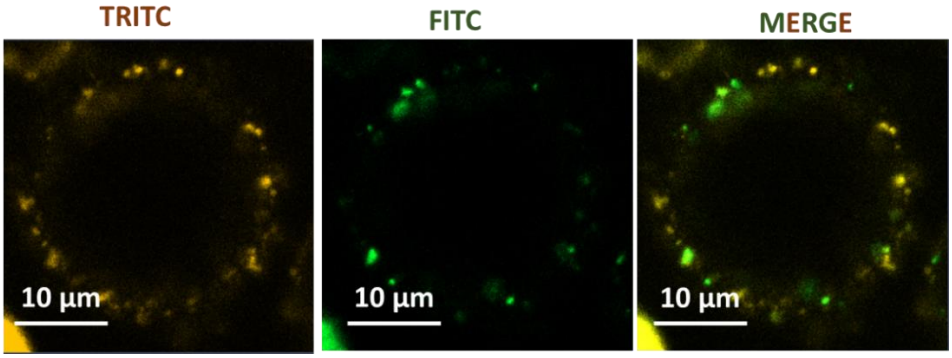

Fig. S24: Representative Two color images of surfactant stabilized o/w interface with GOx-TRITC, ALP-FITC, and untagged HRP in the presence of G-6-P. Experimental condition: [ALP-FITC] = 1 µM, [GOx-TRITC] = 0.5 µM, [HRP] = 0.5 µM, [C_{16}DPA•Zn^{2+}] = 250 µM, [G-6-P] = 1 mM, [1,2-dichlorobenzene] = 20 µl in 980 µl 5mM HEPES buffer pH7 at 25°C.

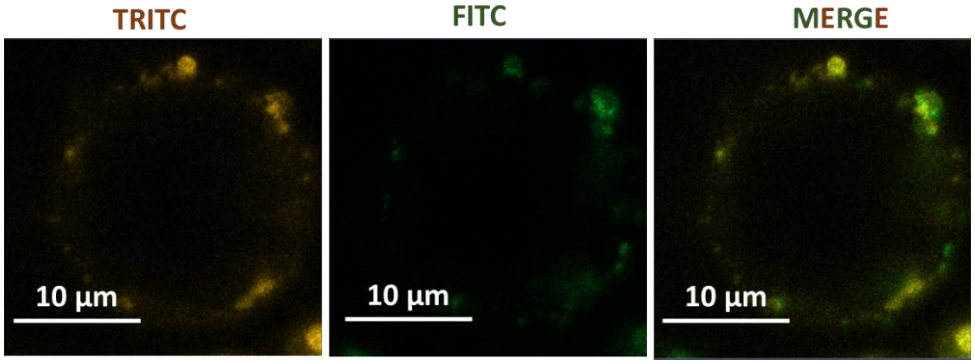

Fig. S25: Representative Two color images of surfactant stabilized o/w interface with GOx-TRITC, ALP-FITC, and untagged HRP in the presence of Glucose and Phosphate. Experimental condition: [ALP-FITC] = 1 µM, [GOx-TRITC] = 0.5 µM, [HRP] = 0.5 µM, [C_{16}DPA•Zn^{2+}] = 250 µM, [Glucose] = 1 mM, [Na_2HPO_4] = 1 mM, [1,2-dichlorobenzene] = 20 µl in 980 µl 5mM HEPES buffer pH7 at 25°C.

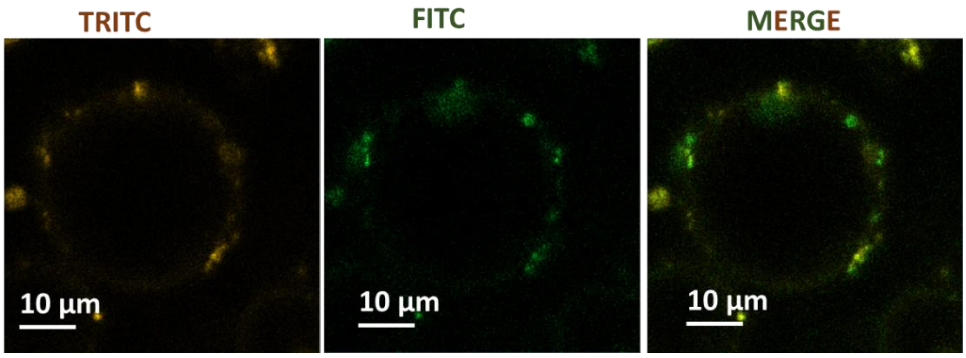

Fig. S26: Representative Two color images of surfactant stabilized o/w interface with GOx-TRITC, ALP-FITC, and untagged HRP in the presence of Phenylphosphate. Experimental condition: [ALP-FITC] = 1 µM, [GOx-TRITC] = 0.5 µM, [HRP] = 0.5 µM, [C_{16}DPA•Zn^{2+}] = 250 µM, [Phenylphosphate] = 1 mM, [1,2-dichlorobenzene] = 20 µl in 980 µl 5mM HEPES buffer pH7 at 25°C.

7. HPNPP catalysis in surfactant stabilized o/w interface:

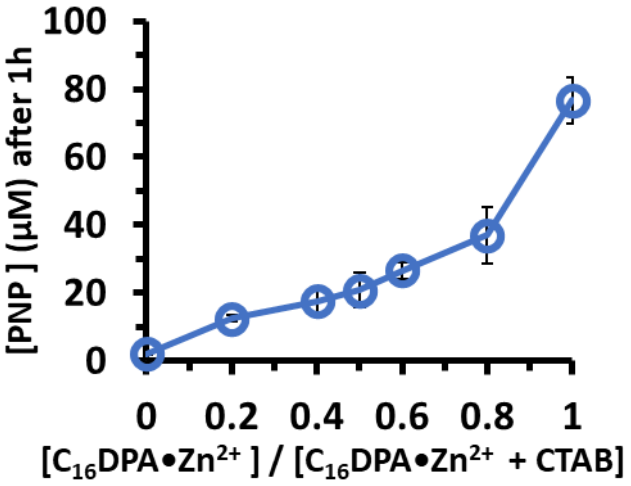

Fig. S27: Representative image of PNP formation as a function of surfactant [C_{16}DPA•Zn^{2+}]/[total surfactant conc.] Concentration ratio from 0-1 at fixed HPNPP concentration of 1 mM, and fixed total concentration of surfactant 250 µM. Here we have used a mixture of surfactant C_{16}DPA•Zn^{2+} and CTAB in the o/w interface to check the catalytic activity of HPNPP. Experimental conditions: [1,2-dichlorobenzene] = 20 µl in 980 µl 5mM HEPES buffer pH7 at 25°C.

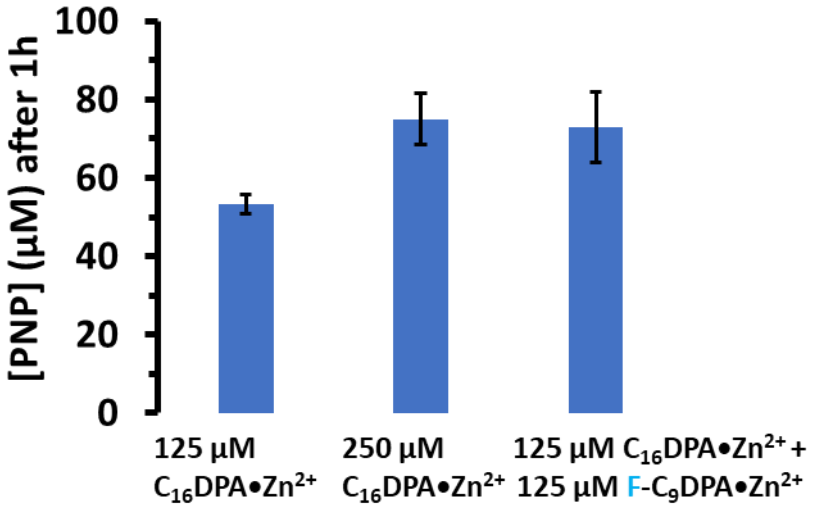

Fig. S28: Representative bar image of PNP formation after 1h in the presence of only 125 µM, 250 µM of $C_{16}DPAZn^{2+}$, and the mixture of 125 µM $C1_6DPA•Zn^{2+}$ + 125 µM F-$C_9DPA•Zn^{2+}$ in the o/w interface. Here we found that the catalytic ability of this fluorophore-containing surfactant was comparable to $C_{16}DPA•Zn^{2+}$ in the o/w droplet. Experimental conditions: [1,2-dichlorobenzene] = 20 µl in 980 µl 5mM HEPES buffer pH7 at 25°C.

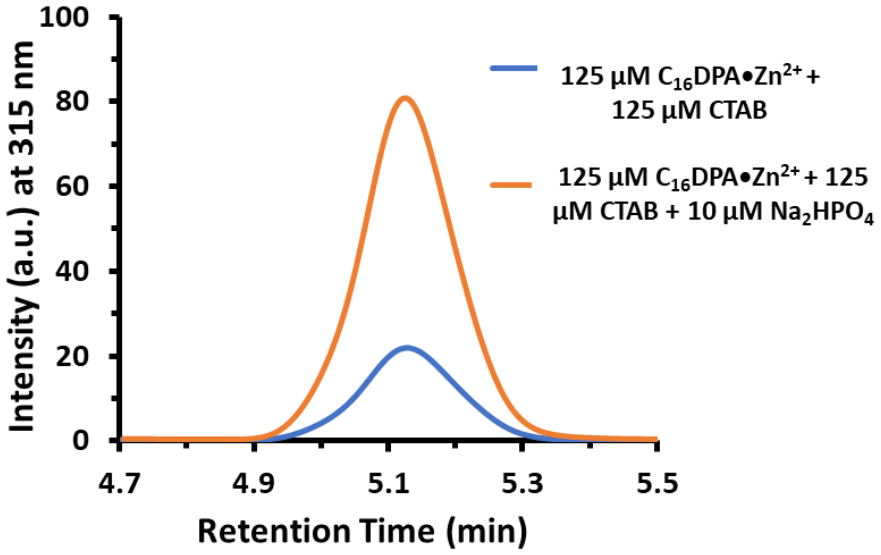

Fig. S29: Representative HPLC Plot of PNP formation after 1h in the presence of 125 µM $C1_6DPA•Zn^{2+}$ + 125 µM CTAB in the o/w interface. Experimental conditions: [1,2-dichlorobenzene] = 20 µl in 980 µl 5mM HEPES buffer pH7 at 25°C.

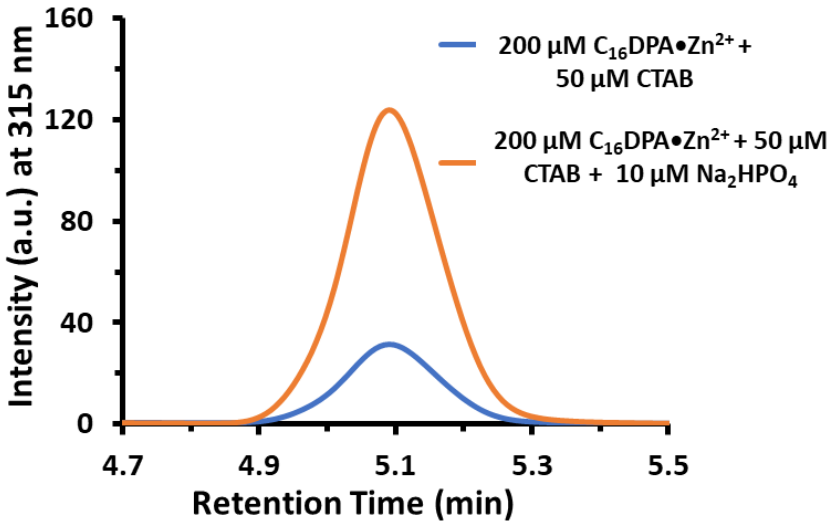

Fig. S30: Representative HPLC Plot of PNP formation after 1h in the presence of 200 µM $C1_6DPA•Zn^{2+}$ + 50 µM CTAB in the o/w interface. Experimental conditions: [1,2-dichlorobenzene] = 20 µl in 980 µl 5mM HEPES buffer pH7 at 25°C.

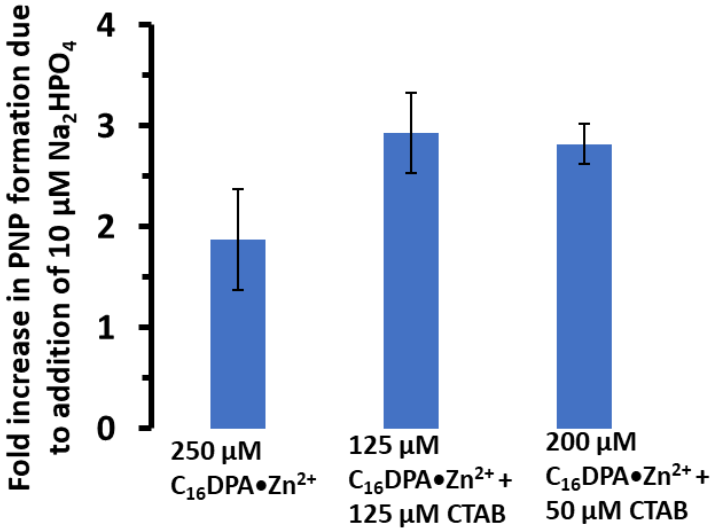

Fig. S31: Representative image of fold increase in PNP formation due to the addition of 10µM Na_2HPO_4 after 1h in the presence of only 250 µM of $C_{16}DPAZn^{2+}$, and the mixture of 125 µM $C1_6DPA•Zn^{2+}$ + 125 µM CTAB, and 200 µM $C_{16}DPA•Zn^{2+}$ + 50 µM CTAB in the o/w interface. Experimental conditions: [1,2-dichlorobenzene] = 20 µl in 980 µl 5mM HEPES buffer pH7 at 25°C.

Table S1 : Table representing the amount of hydrolyzed p-nitrophenol (PNP) formation after 1 hr in the presence of 250 µM $C_{16}DPA•Zn^{2+}$ and different conc. of Na_2HPO_4 in o/w interface.

System	[PNP] (µM) after 1h
250 µM $C_{16}DPA•Zn^{2+}$ + 1 mM HPNPP	76 ± 6.7
250 µM $C_{16}DPA•Zn^{2+}$ + 1 mM HPNPP + 0.01 mM Na_2HPO_4	167 ± 25
250 µM $C_{16}DPA•Zn^{2+}$ + 1 mM HPNPP + 0.1 mM Na_2HPO_4	100 ± 8
250 µM $C_{16}DPA•Zn^{2+}$ + 1 mM HPNPP + 01 mM Na_2HPO_4	6 ± 0.8

Table S2 : Table representing the amount of hydrolyzed p-nitrophenol (PNP) formation after 1 hr in the presence of 250 µM $C_{16}DPA•Zn^{2+}$ and different conc. of NaCl in o/w interface.

System	[PNP] (µM) after 1h
250 µM $C_{16}DPA•Zn^{2+}$ + 1 mM HPNPP	76 ± 6.7
250 µM $C_{16}DPA•Zn^{2+}$ + 1 mM HPNPP + 0.01 mM NaCl	83 ± 10
250 µM $C_{16}DPA•Zn^{2+}$ + 1 mM HPNPP + 0.1 mM NaCl	104 ± 12.5
250 µM $C_{16}DPA•Zn^{2+}$ + 1 mM HPNPP + 1 mM NaCl	78 ± 8.3

8. Fluorescent Microscopic Images of o/w droplet:

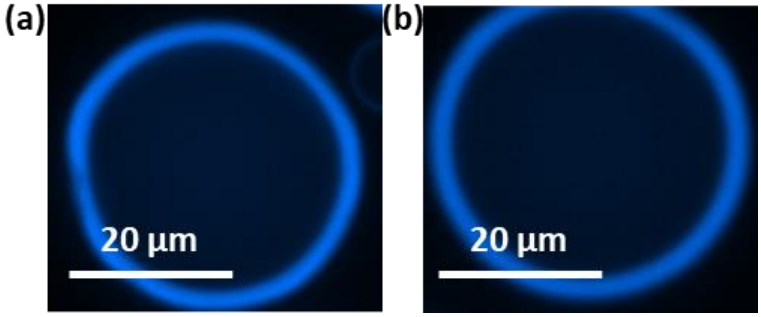

Fig. S32: Fluorescent microscopic images o/w microemulsion where fluorescent but catalytic Zn(II)-metallosurfactant (F-C_9DPA•Zn^{2+}) has been used to probe the surfactant aggregation pattern at the o/w interface in presence of 245 µM C_{16}DPA•Zn^{2+} + 5 µM F-C_9DPA•Zn^{2+}. Experimental conditions: [1,2-dichlorobenzene] = 20 µl in 980 µl 5mM HEPES buffer pH7 at 25°C.

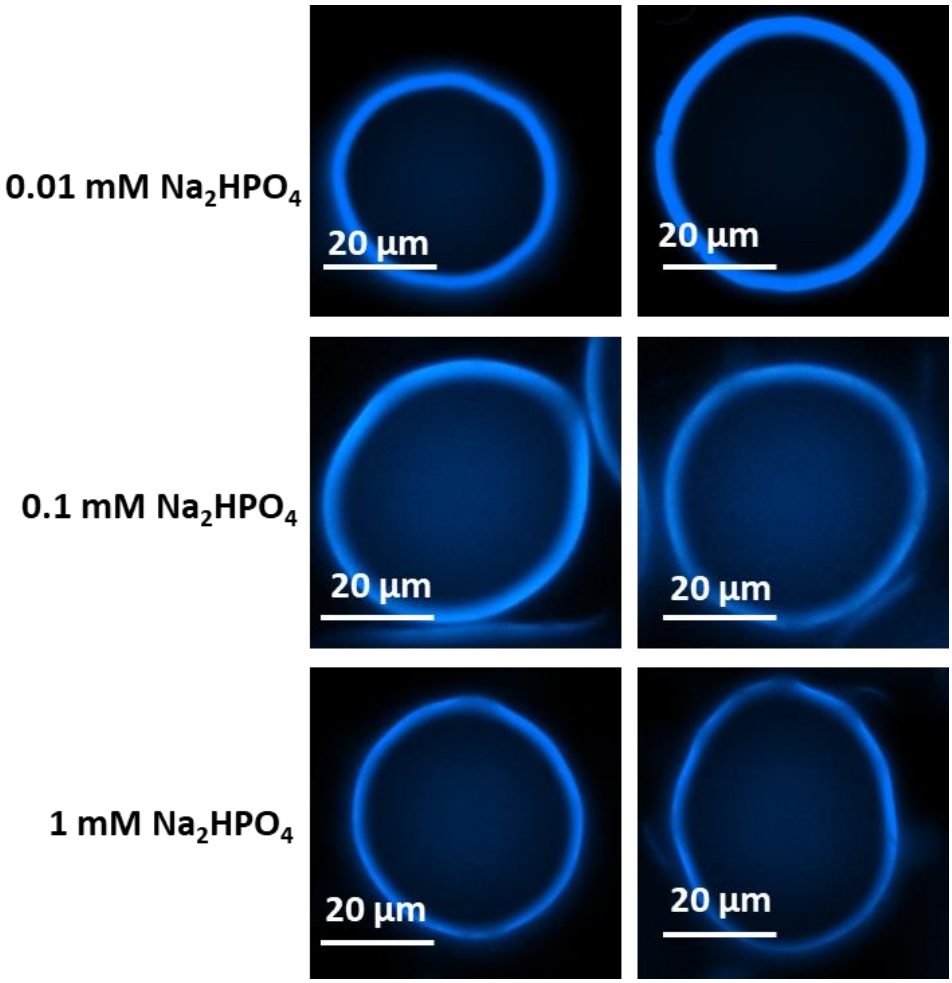

Fig. S33: Fluorescent microscopic images o/w microemulsion where fluorescent but catalytic Zn(II)-metallosurfactant (F-C_9DPA•Zn^{2+}) has been used to probe the surfactant aggregation pattern at the o/w interface in presence of 245 µM C_{16}DPA•Zn^{2+} + 5 µM F-C_9DPA•Zn^{2+} + 1mM HPNPP and different conc. of (0.01 - 1mM) Na_2HPO_4. Experimental conditions: [1,2-dichlorobenzene] = 20 µl in 980 µl 5mM HEPES buffer pH7 at 25°C.

120 µM $C_{16}DPAZn^{2+}$ + 5 µM F-C_9DPAZn^{2+} +125 µM CTAB

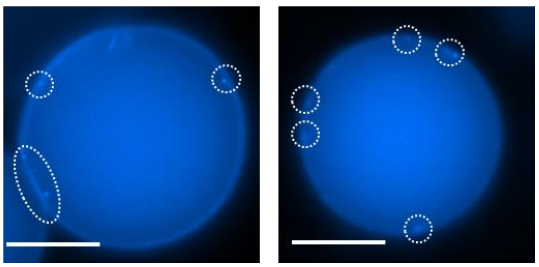

Fig. S34: Fluorescent microscopic images o/w microemulsion where fluorescent but catalytic Zn(II)-metallosurfactant (F-$C_9DPA•Zn^{2+}$) has been used to probe the surfactant aggregation pattern at the o/w interface in presence of 120 µM $C_{16}DPA•Zn^{2+}$ + 5 µM F-$C_9DPA•Zn^{2+}$ + 125 µM CTAB. Experimental conditions: [1,2-dichlorobenzene] = 20 µl in 980 µl 5mM HEPES buffer pH7 at 25°C. Scale bar here is 20 µm.

120 µM $C_{16}DPAZn^{2+}$ + 5 µM F-C_9DPAZn^{2+} +125 µM CTAB+ 1 mM HPNPP

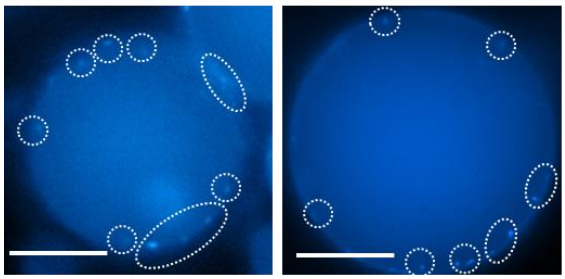

Fig. S35: Fluorescent microscopic images o/w microemulsion where fluorescent but catalytic Zn(II)-metallosurfactant (F-$C_9DPA•Zn^{2+}$) has been used to probe the surfactant aggregation pattern at the o/w interface in presence of 120 µM $C_{16}DPA•Zn^{2+}$ + 5 µM F-$C_9DPA•Zn^{2+}$ + 125 µM CTAB + 1 mM HPNPP. Experimental conditions: [1,2-dichlorobenzene] = 20 µl in 980 µl 5mM HEPES buffer pH7 at 25°C. Scale bar here is 20 µm.

120 µM $C_{16}DPAZn^{2+}$ + 5 µM F-C_9DPAZn^{2+} +125 µM CTAB+ 1 mM HPNPP+ 0.01 mM Na_2HPO_4

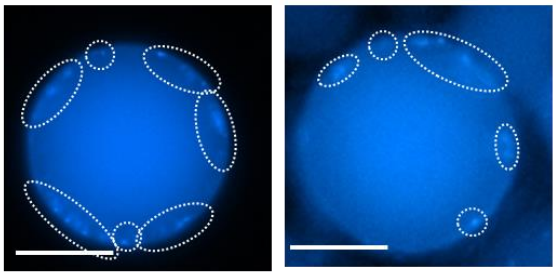

Fig. S36: Fluorescent microscopic images o/w microemulsion where fluorescent but catalytic Zn(II)-metallosurfactant (F-$C_9DPA•Zn^{2+}$) has been used to probe the surfactant aggregation pattern at the o/w interface in presence of 120 µM $C_{16}DPA•Zn^{2+}$ + 5 µM F-$C_9DPA•Zn^{2+}$ + 125 µM CTAB + 1 mM HPNPP + 0.01 mM Na_2HPO_4. Experimental conditions: [1,2-dichlorobenzene] = 20 µl in 980 µl 5mM HEPES buffer pH7 at 25°C. The scale bar here is 20 µm.

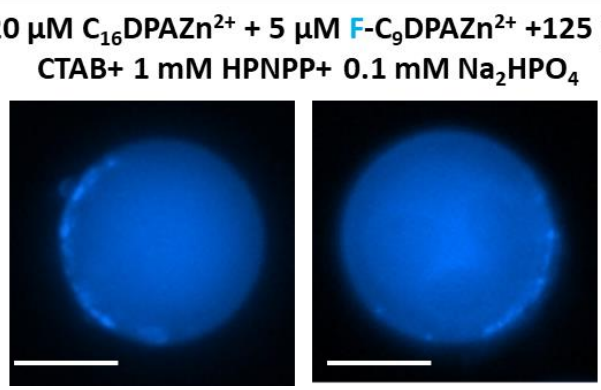

Fig. S37: Fluorescent microscopic images o/w microemulsion where fluorescent but catalytic Zn(II)-metallosurfactant (F-C_9DPA•Zn^{2+}) has been used to probe the surfactant aggregation pattern at the o/w interface in presence of 120 µM C_{16}DPA•Zn^{2+} + 5 µM F-C_9DPA•Zn^{2+} + 125 µM CTAB + 1 mM HPNPP + 0.1 mM Na_2HPO_4. Experimental conditions: [1,2-dichlorobenzene] = 20 µl in 980 µl 5mM HEPES buffer pH7 at 25°C. The scale bar here is 20 µm.

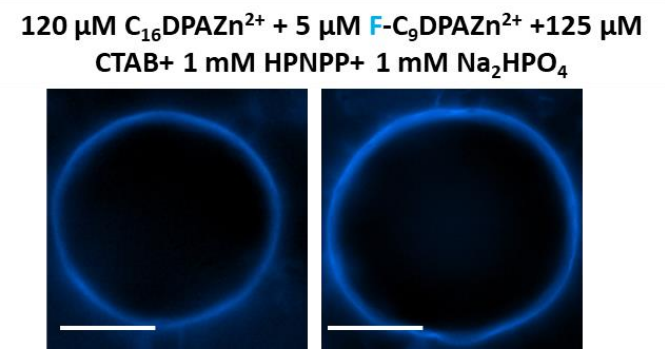

Fig. S38: Fluorescent microscopic images o/w microemulsion where fluorescent but catalytic Zn(II)-metallosurfactant (F-C_9DPA•Zn^{2+}) has been used to probe the surfactant aggregation pattern at the o/w interface in presence of 120 µM C_{16}DPA•Zn^{2+} + 5 µM F-C_9DPA•Zn^{2+} + 125 µM CTAB + 1 mM HPNPP + 1 mM Na_2HPO_4. Experimental conditions: [1,2-dichlorobenzene] = 20 µl in 980 µl 5mM HEPES buffer pH7 at 25°C. The scale bar here is 20 µm.

In this case, the band is like only metallosurfactant-doped o/w droplet as shown in Fig. S33, ESI. It is due to the presence of more phosphate which binds strongly with the metallosurfactant resulting an almost homogeneous interface. However, the band width or intensity is lower in this case as the amount of metallosurfactant is two-times lower than the previous one (Fig. S33).

9. **Supporting Videos**:

Videos showing clustering of metallosurfactant in the presence of substrate HPNPP or HPNPP + P_i recorded with 100x objective after 2 minutes of drop-casting the solution on the glass slide (played at 2x speed of the original recorded video).

Experimental condition: **For Supporting Video S1**, this video shows control experiment of clustering of metallosurfactant in absence of substrate HPNPP or HPNPP + P_i. [C_{16}DPA•Zn^{2+}] = 120 µM, [F-C_9DPA•Zn^{2+}] = 5 µM, [CTAB] = 125µM, [1,2-dichlorobenzene] = 20 µl in 980 µl 5mM HEPES buffer pH7 at 25°C.

For Supporting Video S2, this video shows clusters of metallosurfactant in presence of substrate HPNPP. [C_{16}DPA•Zn^{2+}] = 120 µM, [F-C_9DPA•Zn^{2+}] = 5 µM, [CTAB] = 125µM, [HPNPP] = 1 mM, [1,2-dichlorobenzene] = 20 µl in 980 µl 5mM HEPES buffer pH7 at 25°C.

For Supporting Video S3, this video shows clusters of metallosurfactant in presence of substrate HPNPP + P_i. [C_{16}DPA•Zn^{2+}] = 120 µM, [F-C_9DPA•Zn^{2+}] = 5 µM, [CTAB] = 125µM, [HPNPP] = 1 mM, [Na_2HPO_4] = 0.01 mM, [1,2-dichlorobenzene] = 20 µl in 980 µl 5mM HEPES buffer pH = 7 at 25°C.

10. References:

[S1] Priyanka, S. Kaur Brar and S. Maiti, *ChemNanoMat*, 2022, **8**, e202100498.

[S2] Aastha, Priyanka and S. Maiti, *Chem. Commun*., 2023, **59**, 6536–6539.

[S3] D. V. Kachkin, V. V. Lashkul, N. A. Gorsheneva, S. A. Fedotov, M. S. Rubel, Y. O. Chernoff and A. A. Rubel, *Int. J. Mol. Sci.*, 2023, **24**, 14122.